Title

From the Cover: BDE-47 and BDE-49 Inhibit Axonal Growth in Primary Rat Hippocampal Neuron-Glia Co-Cultures via Ryanodine Receptor-Dependent Mechanisms

Journal

Toxicological Sciences, 156(2)

ISSN

1096-6080

Authors

Chen, Hao

Streifel, Karin M

Singh, Vikrant

et al.

Publication Date

2017-04-01

DOI

10.1093/toxsci/kfw259

Peer reviewed

BDE-47 and BDE-49 Inhibit Axonal Growth in Primary Rat Hippocampal Neuron-Glia Co-Cultures via Ryanodine Receptor-Dependent Mechanisms

Hao Chen*, Karin M. Streifel*, Vikrant Singh†, Dongren Yang*, Linley Mangini*, Heike Wulff†, and Pamela J. Lein*‡

*Department of Molecular Biosciences, School of Veterinary Medicine, University of California-Davis, Davis, CA 95616; haochen@ucdavis.edu; karin.streifel@gmail.com; lmmangini@ucdavis.edu; pjlein@ucdavis.edu; †Department of Pharmacology, School of Medicine, University of California-Davis, Davis, CA 95616; vssingh@ucdavis.edu; hwulff@ucdavis.edu

‡Corresponding author: Pamela J. Lein, PhD
Molecular Biosciences, School of Veterinary Medicine
University of California, Davis
1089 Veterinary Medicine Drive
Davis, CA 95616
E-mail: pjlein@ucdavis.edu
Tel: (530) 752-1970
Fax: (530) 752-7690

Running Title: PBDEs inhibit axonal growth *in vitro*

Abstract (limit is 250 words, currently at 250 words)

Polybrominated diphenyl ethers (PBDEs) are widespread environmental contaminants associated with adverse neurodevelopmental outcomes in children and preclinical models; however, the mechanisms by which PBDEs cause developmental neurotoxicity remain speculative. The structural similarity between PBDEs and non-dioxin-like (NDL) polychlorinated biphenyls (PCBs) suggests shared toxicological properties. Consistent with this, both NDL PCBs and PBDEs have been shown to stabilize ryanodine receptors (RyRs) in the open configuration. NDL PCB effects on RyR activity are causally linked to increased dendritic arborization, but whether PBDEs similarly enhance dendritic growth is not known. In this study, we quantified the effects of individual BDE congeners on not only dendritic but also axonal growth since both are regulated by RyR-dependent mechanisms, and both are critical determinants of neuronal connectivity. Primary neuronal-glial co-cultures dissociated from the neonatal rat hippocampus were exposed to BDE-47 or BDE-49 in the culture medium at concentrations ranging from 20 pM to 2 μM. At these concentrations, neither PBDE congener altered dendritic arborization. In contrast, at concentrations ≥ 200 pM, both congeners delayed neuronal polarization resulting in significant inhibition of axonal outgrowth during the first few days *in vitro*. The axon inhibitory effects of these PBDE congeners occurred independent of cytotoxicity, and were blocked by pharmacological antagonism of RyR or siRNA knockdown of RyR2. These results demonstrate that the molecular and cellular mechanisms by which PBDEs interfere with neurodevelopment overlap with but are distinct from those of NDL PCBs, and suggest that altered patterns of neuronal connectivity may contribute to the developmental neurotoxicity of PBDEs.

Keywords: axon, calcium signaling, developmental neurotoxicity, neuronal morphogenesis, PBDE, ryanodine receptor

Introduction (750 word limit, currently at 655 words)

Polybrominated diphenyl ethers (PBDEs), synthetic brominated compounds that were used extensively as flame retardants in consumer products, have become persistent and ubiquitous environmental contaminants. PBDE levels in human tissues have increased significantly over the past three decades (EFSA, 2011; USEPA, 2010), and body burdens are significantly higher in infants and toddlers relative to adults (Lunder *et al.*, 2010; She *et al.*, 2007; Toms *et al.*, 2009). Epidemiological studies report an association between early-life PBDE exposure and neurobehavioral deficits, including decreased attention, poorer performance on intelligence indices, psychomotor deficits and increased activity/impulsivity (Chao *et al.*, 2011; Eskenazi *et al.*, 2013; Gascon *et al.*, 2012; Herbstman *et al.*, 2010; Hoffman *et al.*, 2012; Roze *et al.*, 2009; Shy *et al.*, 2011). Preclinical studies confirm that developmental PBDE exposures can cause persistent neurobehavioral deficits (Costa *et al.*, 2014; Hendriks and Westerink, 2015).

PBDEs have been reported to interfere with thyroid hormone function, alter Ca^{2+} homeostasis, cause oxidative stress and modulate cholinergic, glutamatergic and GABAergic neurotransmission (Costa et al., 2014; Dingemans *et al.*, 2011; Hendriks and Westerink, 2015). However, it is not clear whether or how these molecular effects relate to PBDE-induced neurobehavioral deficits. One hypothesis is that PBDEs cause developmental neurotoxicity by interfering with normal patterns of neuronal connectivity (Kodavanti and Curras-Collazo, 2010; Stamou *et al.*, 2013). This hypothesis is derived from the following observations: *(1)* thyroid hormone, Ca^{2+}, reactive oxygen species (ROS) and neurotransmitter-dependent signaling mechanisms are well known to influence the development of neuronal connectivity via dynamic control of axonal and dendritic morphogenesis (Chandrasekaran *et al.*, 2015; Goldberg, 2003; Kapfhammer, 2004; Lohmann and Wong, 2005; Valnegri *et al.*, 2015); and *(2)* dysregulated axonal or dendritic growth is linked to impaired behavior in preclinical models (Berger-Sweeney and Hohmann, 1997), and to multiple neurodevelopmental disorders in humans, including

78 autism spectrum disorders, attention deficit hyperactivity disorder and schizophrenia (Copf,
79 2016; Robichaux and Cowan, 2014).
80 In further support of this hypothesis, we previously demonstrated that PBDE congeners with
81 more than one *ortho* bromine substitution interact with the ryanodine receptor (RyR) to promote
82 Ca^{2+} release from intracellular stores (Kim *et al.*, 2011). RyRs are Ca^{2+} channels that regulate
83 Ca^{2+} release from the endoplasmic reticulum (Pessah *et al.*, 2010), and RyR function is required
84 for activity-dependent dendritic growth (Adasme *et al.*, 2011; Ohashi *et al.*, 2014; Wayman *et*
85 *al.*, 2012b) and for axonal growth and guidance (Arie *et al.*, 2009; Gomez *et al.*, 1995;
86 Jacques-Fricke *et al.*, 2006; Ooashi *et al.*, 2005). Nanomolar concentrations of non-dioxin-like
87 (NDL) polychlorinated biphenyls (PCBs), which are structurally similar to PBDEs and proposed
88 to share toxicological modes of action (Kodavanti and Curras-Collazo, 2010), also interact with
89 RyR1 and RyR2 to sensitize their activation by submicromolar levels of Ca^{2+} and attenuate their
90 inhibition by micromolar levels of Ca^{2+} and Mg^{2+} (Wong *et al.*, 1997a; Wong and Pessah, 1996).
91 NDL PCB interactions with RyR stabilize the receptor in its open configuration (Samso *et al.*,
92 2009), which increases intracellular levels of Ca^{2+} (Wayman *et al.*, 2012a). NDL PCB
93 sensitization of RyRs is causally linked to enhanced dendritic arborization in hippocampal and
94 cortical neurons (Wayman et al., 2012b; Yang *et al.*, 2014; Yang *et al.*, 2009) via activation of
95 Ca^{2+}-dependent signaling pathways (Wayman et al., 2012a). While PBDEs were recently
96 reported to alter axonal growth in larval zebrafish (Chen *et al.*, 2012), whether PBDEs influence
97 axonal or dendritic morphogenesis in mammalian central neurons via RyR-dependent
98 mechanisms has not been previously evaluated.
99 Here, we address this question by exposing primary cultures of rat hippocampal neurons to
100 either BDE-47, a PBDE congener with weak RyR activity (Kim et al., 2011) that is highly
101 abundant in human tissues (USEPA, 2010), or BDE-49, a PBDE congener with potent RyR
102 activity (Kim et al., 2011) that has been detected in gestational tissues from women in southeast
103 Michigan at levels comparable to BDE-47 (Miller *et al.*, 2009). Our findings indicate that while

neither congener alters dendritic arborization, both decrease axonal growth with comparable potency via RyR-dependent mechanisms.

Materials and Methods

Materials

Neat certified BDE-47 (2,2',4,4'-tetrabromodiphenyl ether, > 99% pure) and BDE-49 (2,2',4,5'-tetrabromodiphenyl ether, > 99% pure) were purchased from AccuStandard Inc. (New Haven, CT), and verified for purity and composition by GC/MS by the UC Davis Superfund Research Program Analytical Core. Stock solutions of each BDE were made in dry dimethyl sulfoxide (DMSO, Sigma-Aldrich, St. Louis, MO). Paraformaldehyde was purchased from Sigma-Aldrich. FLA365 (4-(2-aminopropyl)-3,5-dichloro-*N,N*-dimethylaniline) was synthesized as previously described (Florvall *et al.*, 1977) and confirmed to be > 99% pure by NMR (see Supplemental File 1). Xestospongin C was purchased from Cayman Chemical (Ann Arbor, MI); verapamil, from Sigma-Aldrich. MAP2B-eGFP and pCAG-tomato fluorescent protein (TFP) constructs were generous gifts from Dr. Gary Wayman (Washington State University, Pullman, WA) and their synthesis and characterization have been previously published (Wayman *et al.*, 2006).

Animals

All procedures involving animals were conducted according to protocols approved by the Institutional Animal Care and Use Committee of the University of California, Davis. Timed-pregnant Sprague Dawley rats were purchased from Charles River Laboratory (Hollister, CA) and individually housed in clear plastic cages with corn cob bedding. Food and water were provided *ad libitum*. Temperatures were maintained at 22 ± 2 ˚C throughout a 12 h light-dark cycle.

130 ***Cell Culture***

131 Primary hippocampal cell cultures were prepared from postnatal day (P) 0 or P1 male and
132 female rat pups (hippocampi from male and female pups were pooled) as previously described
133 (Wayman et al., 2006). Briefly, dissociated hippocampal cells were plated on glass coverslips
134 (Bellco Glass, Vineland, NJ) precoated with poly-L-lysine (0.5 mg/mL, Sigma-Aldrich) and
135 maintained at 37˚C in NeuralQ Basal Medium supplemented with 2% GS21 (MTI-GlobalStem,
136 Gaithersburg, MD) and GlutaMAX (ThermoScientific, Waltham, MA). For studies of neuronal cell
137 polarization, axonal morphogenesis and intracellular Ca^{2+} levels, cells were plated at 33,000
138 cells/cm^2; for studies of dendritic growth, at 83,000 cells/cm^2. Phase contrast images of cultures
139 grown at either cell density are provided in Supplemental Figure 2. For all PBDE exposure
140 experiments, cultures were exposed to varying concentrations of BDE-47 or BDE-49 diluted in
141 culture medium from 1000X stocks; control cultures were exposed to vehicle (DMSO; 1:1000
142 dilution). For studies of neuronal cell polarization, axonal growth and intracellular Ca^{2+} levels,
143 cultures were exposed for 48 h beginning 3 h after plating; for dendritic growth studies, cultures
144 were exposed for 48 h beginning on day *in vitro* (DIV) 7.
145
146 ***siRNA Knockdown***

147 Construct sequences and specificity of RyR1 siRNA, RyR2 siRNA and control (scrambled)
148 siRNA were previously published (Wayman et al., 2012b). In this study, siRNA were
149 fluorescently labeled using LabelIT® (Mirus, Madison WI) per the manufacturer's instructions in
150 order to identify transfected cells. To transfect hippocampal neurons, freshly dissociated
151 hippocampal cells were electroporated with siRNA prior to plating using the Amaxa Nucleofector
152 (Amaxa Biosystems, Lonza) according to the manufacturer's protocol. Transfection efficiency
153 was approximately 40%.
154
155

Morphometric analyses

To visualize the dendritic arbor, hippocampal cultures were transfected on DIV 6 with a pCAGGS expression vector encoding a microtubule-associated protein-2B (MAP2B)-enhanced green fluorescent protein (eGFP) fusion construct (Wayman et al., 2006), using Lipofectamine-2000 (Invitrogen, Carlsbad, CA) according to the manufacturer's protocol. Transfection efficiency ranged between Dendritic lengths were quantified from digital images of GFP+ neurons using ImageJ software with the NeuronJ plugin (Meijering *et al.*, 2004) by an individual blinded to experimental condition. Total dendritic length was measured in at least 30 neurons from 3 coverslips per treatment group, and the experiment was repeated at least three times with cultures prepared from independent dissections.

To quantify axonal morphology, cultures were fixed with 4% paraformaldehyde then reacted with antibody specific for Tau-1 (1:1000, Millipore, Billerica, MA) to visualize axons. Axonal lengths were quantified in Tau-1 immunopositive neurons by an individual blinded to experimental condition using ImageJ software with the NeuronJ plugin. As previously defined (Dotti *et al.*, 1988; Lein *et al.*, 1992), a neurite was considered an axon if its length was at least 2.5 times the diameter of the cell body, and it exceeded in length all other neurites extended by the same neuron. Total axonal length was measured in at least 30 neurons from 3 coverslips per treatment group, and the experiment was repeated in cultures prepared from three independent dissections.

To assess neuronal cell polarity, cultures were reacted with GAP-43 antibody (1:1000, Millipore, Billerica, MA). Polarity was scored in GAP-43 immunopositive neurons by an individual blinded to treatment using previously described stages (Goslin *et al.*, 1990). The experiment was repeated in cultures prepared from three independent dissections.

Cytotoxicity Analyses

Cytotoxicity was assessed by quantifying lactate dehydrogenase (LDH) released into the culture medium (Mosmann, 1983) using the CytoTox-ONE™ Homogenous Membrane Integrity Assay (Promega, Madison, WI, USA) per the manufacturer's directions. Cell viability was also assessed in independent cultures by reacting cultures with calcein-AM (0.25 μM; Invitrogen) and propidium iodide (1.25 μM; Sigma-Aldrich) to identify live and dead cells, respectively. The percentage of live (calcein-AM labeled) versus dead (propidium iodide-labeled) cells in each culture was determined using an automated high content imaging system (ImageExpress, Molecular Devices, Sunnyvale, CA). Cytotoxicity was assayed in 12 wells per treatment and experiments were repeated using cultures obtained from three independent dissections.

Western blot analysis of tau-1

At DIV 5, low density cultures were treated with BDE-47 or BDE-49 for 48 h, then lysed with ice-cold RIPA buffer (150 mM NaCl, 1.0% NP-40, 0.5% sodium deoxycholate, 0.1% SDS in 50 mM Tris, pH 8.0 with Halt protease inhibitor). Protein concentrations of the lysates were determined using the BCA Protein Assay (Pierce, Rockford IL). An equal amount of protein (10 μg) of each sample was separated by 12% SDS-PAGE, and transferred to PDVF membrane. Membranes were blocked for 1 h in Odyssey Blocking Buffer (LI-COR, Lincoln NE) then incubated overnight with antibodies specific for tau-1 (1:1000, Millipore, Billerica, MA) and GAPDH (1:1000, Cell Signaling Technology Danvers, MA) prepared in blocking buffer. After PBS wash, membranes were incubated with secondary antibodies conjugated to infrared dye IR700 or IR800 for 1 h and then washed with PBS. Membranes were scanned and densitometric values obtained using the Odyssey Infrared Imaging System (LI-COR, Lincoln NE). The densitometric value for each tau-1 immunopositive band was normalized to the densitometric value for the GAPDH immunopositive band within the same sample.

Calcium Imaging

Spontaneous Ca^{2+} transients were measured in dissociated hippocampal cells cultured on CoStar® 96-well plates (Corning Inc, Corning, NY). At DIV 2, cells were loaded with the Ca^{2+}-sensitive dye Fluo-4 AM (4 µM; Invitrogen) in Locke's buffer (8.6 mM 4-(2-hydroxyethyl)-1-piperazineethanesulfonic acid, 5.6 mM KCl, 154 mM NaCl, 5.6 mM glucose, 1.0 mM $MgCl_2$, 2.3 mM $CaCl_2$, and 0.0001 mM glycine, pH 7.4) at 37°C for 30 min. Cultures were washed with Locke's Buffer and transferred to the ImageXpress Micro XLS high content imaging system. The temperature was maintained at 37˚C throughout the recording period. Fluorescence was recorded every 15 s over the 26 min experiment. After 5 min of baseline recording, vehicle, BDE-47 or BDE-49 was added to the cultures and data captured for an additional 20 min. At the conclusion of the 20 min recording, viable neurons were identified by adding 30 mM KCl to the medium to depolarize neurons; any neurons that did not respond with a transient Ca^{2+} spike were not included in the subsequent analyses. The transient amplitude of Ca^{2+} fluorescence was measured by normalizing peak change in Fluo-4 AM fluorescence (ΔF) to the baseline fluorescence (F0) and presented as the mean ΔF/F0 per neuron. Area under the curve (AUC) measurements were calculated via the trapezoid method using Graphpad Prism version 4.0 (San Diego, CA). Baseline levels were held constant at zero and peaks less than 10% of total amplitude were excluded. Levels of calcium flux within each cell were collected throughout the experimental time from all treatments. Within each field of view, > 30 cells were identified for analysis; 1 field was imaged per well in 2 wells per experimental group. Statistical comparisons were made on mean values per group with cultures obtained from four independent dissections (e.g., N=4 per group).

Immunocytochemical localization of RyR

To confirm RyR expression in the axonal growth cone, cultures were fixed with 4% paraformaldehyde on DIV 2, permeabilized with 0.1% Triton X-100 for 5 min, incubated in

blocking buffer containing 5% fetal bovine serum, 0.05 M NH_4Cl, 2% glycerol, and 2% goat serum for 1 h and then reacted overnight with RyR1-selective antibody 34C (1:100, Developmental Studies Hybridoma Bank, Iowa City, IA) or RyR2-selective antibody C3-33 (1:100, Abcam, Cambridge, MA). After PBS wash, Alexa Fluor dyes (1:1000, Molecular Probes, Invitrogen) and Oregon-Green phalloidin (1:1000, ThermoScientific) were applied for 1 h.

Statistical analysis

All data are presented as mean ± SE. Graphs and statistical analyses were performed with GraphPad Prism 4.0. Data were analyzed using one-way *ANOVA* with Tukey's or Dunnett's *post-hoc* or with Kruskal-Wallis with Dunn's *post-hoc* as appropriate. Datasets were log transformed for statistical analysis if they did not pass the Shapiro-Wilk test of normality.

Results

BDE-47 and BDE-49 selectively interfere with axonal growth in primary hippocampal neurons

We have previously shown that RyR-active NDL-PCBs enhance dendritic arborization in cultured hippocampal neurons (Wayman et al., 2012b; Yang et al., 2014). Therefore, we initially predicted that BDE-47 and BDE-49, which exhibit relatively low versus relatively high RyR activity, respectively (Kim et al., 2011), would exhibit weak versus robust dendrite promoting activity. To visualize dendritic arbors of individual neurons in high-density neuron-glia co-cultures dissociated from P0-P1 rat hippocampi, cultures were transfected with a MAP2B-EGFP construct under the control of the neuron-specific *CAG* promoter (Wayman et al., 2006). Expression of MAP2B-eGFP is restricted to the somatodendritic compartment in cultured hippocampal neurons and does not alter their intrinsic dendritic growth patterns (Wayman et al., 2006). Under the culture conditions used for these experiments, the dendritic arbor expands most rapidly between DIV 5-10 (Wayman et al., 2006); therefore, cultures were transfected with

MAP2B-eGFP on DIV 6, then exposed from DIV 7-9 to varying concentrations of BDE-47 or BDE-49. Control cultures were exposed to vehicle (DMSO at 1:1000 dilution) or, as a positive control, to PCB 95 (200 nM). PCB 95 is a NDL-PCB with potent activity at the RyR that we previously demonstrated significantly enhances dendritic arborization in cultured hippocampal neurons (Wayman et al., 2012b). Consistent with previous studies (Wayman et al., 2012b), neurons exposed to PCB 95 had a more complex dendritic arbor (Figure 1A), evidenced as a significant increase in total dendritic length per neuron relative to vehicle control neurons (Figure 1B). In contrast, the dendritic arborization of neurons exposed to either BDE-47 or BDE-49 at concentrations ranging from 200 pM to 2 μM was not significantly different from that of neurons exposed to vehicle (Figure 1A, B).

RyRs are expressed not only in dendrites (Seymour-Laurent and Barish, 1995; Wayman et al., 2012b), but also in axons (Hertle and Yeckel, 2007), and RyR activity has been implicated in the regulation of axonal growth and guidance (Ooashi et al., 2005; Welshhans and Rehder, 2007). Therefore, we examined whether PBDEs alter axonal growth in primary hippocampal neurons. For studies of axonal growth, primary hippocampal cell cultures were plated at a lower cell density and exposed to BDE-47 or BDE-49 for 48 h beginning 3 h after plating in order to visualize the complete axonal plexus of individual neurons (Yang et al., 2014). At the end of the exposure period, cultures were fixed and immunostained for tau-1, which is an axon-selective cytoskeleton-associated protein (Hayashi *et al.*, 2002). Exposure to either BDE-47 or BDE-49 did not change the number of axons extended by cultured hippocampal neurons but did significantly decrease the length of axons (Figure 2A). Morphometric analyses indicated that at concentrations ranging from 200 pM to 2 μM, both PBDE congeners significantly decreased axonal length by 15-25% relative to vehicle control values (Figure 2B). Exposure to BDE-47 or BDE-49 at 20 pM did not significantly alter axonal length relative to vehicle controls.

To determine whether PBDE effects on axonal growth are a secondary effect of cytotoxicity, cell viability was assessed in PBDE-exposed cultures using two assays that measure different

parameters of cell health: LDH release (Lobner, 2000) and cellular uptake of calcein AM and propidium iodide (Vaughan *et al.*, 1995). Under the same culture conditions and PBDE exposure paradigms used for axonal growth studies, neither BDE-47 nor BDE-49 significantly altered LDH release (Figure 3A) or calcein AM and propidium iodide uptake (Figure 3B) relative to vehicle controls.

To determine whether the differential effects of BDE-47 and BDE-49 on axonal *vs*. dendritic growth reflect differential susceptibility of immature (DIV 2) *vs*. more mature (DIV 7-9) cell cultures, respectively, we tested the effects of these PBDE congeners on axonal growth following the same exposure paradigm used for the dendritic growth assay. Because it is technically challenging to quantify axonal lengths of individual neurons in mature cultures using morphometric analyses, we used western blotting to quantify expression levels of the axon-selective cytoskeletal protein tau-1 in hippocampal cultures exposed to BDE-47 or BDE-49 from DIV 7-9. Levels of tau-1 protein in BDE-exposed cultures were not significantly different from those in vehicle control cultures (Figure 4).

The observation that PBDEs did not significantly alter tau-1 expression in mature neurons but did decrease axonal length in immature neurons (Figure 2) suggests that these compounds interfere with very early events of axonal morphogenesis in hippocampal neurons. Previous studies have shown that hippocampal neurons in culture undergo a well-defined sequence of morphological changes to transition from an unpolarized cell with multiple “minor” neurites that are neither axonal or dendritic into the characteristic polarized neuron with a single axonal process and multiple dendrites (Dotti et al., 1988). Polarization of these neurons typically occurs over the first 24-48 h in culture, and is marked by the differentiation of one of multiple “minor” neurites into a definable axon (Wiggin *et al.*, 2005). To assess whether PBDE effects on axon length were mediated by changes in the rate of neuronal cell polarization, hippocampal cell cultures were immunostained for GAP-43, a biomarker of axonal growth cones (Goslin and Banker, 1990; Goslin et al., 1990). To score the different stages of neuronal cell polarization,

we used previously described criteria based on neuronal cell morphology and the subcellular distribution of GAP-43 immunoreactivity (Goslin and Banker, 1990; Goslin et al., 1990; Harrill *et al.*, 2013). Briefly, polarization was scored as Stage 1 if GAP-34 immunoreactivity was localized to the cell body with no discernable immunostaining of neurites; Stage 2, if GAP-43 immunoreactivity was obvious in all neurites and no one neurite was significantly longer than the others; or Stage 3, if GAP-43 immunoreactivity was most robust in the growth cone of a single neurite that was significantly longer than the remaining neurites (Figure 5A). Stage 3 marks the initial polarization of the neuron when the GAP-43 immunopositive neurite becomes the axon (Dotti et al., 1988; Goslin and Banker, 1990). Under the culture conditions used for our studies of PBDE effects on axonal growth, the majority of neurons (> 75%) reached Stage 3, or become polarized, within 48 h after plating (Figure 5B). Therefore, in experiments examining the effects of PBDE exposure on neuronal cell polarization, we examined cultures at DIV 2. In cultures exposed to either BDE-47 or BDE-49 at 200 nM for 48 h beginning 3 h after plating, there were significantly fewer neurons that had reached stage 3 (or become polarized) by DIV 2 relative to vehicle control cultures (Figure 5C).

PBDE effects on axonal growth are mediated by RyR-dependent mechanisms

Cytosolic Ca^{2+} plays an important role in axonal growth and guidance (Zheng and Poo, 2007). Since it has previously been shown that PBDEs disrupt Ca^{2+} homeostasis (Dingemans *et al.*, 2010b; Dingemans et al., 2011; Kim et al., 2011), we hypothesized that PBDE effects on axonal growth are mediated by changes in intracellular Ca^{2+} levels ($[Ca^{2+}]_i$). To test this hypothesis, hippocampal neurons at DIV 2 were acutely exposed to vehicle or concentrations of BDE-47 or BDE-49 that inhibit axonal growth. At 2 nM or 2 μM, neither PBDE congener elicited changes in $[Ca^{2+}]_i$ that were detectable using high content imaging of cells loaded with Fluo-4 AM (Supplemental file 3). To confirm that our approach was sensitive enough to detect previously reported changes in $[Ca^{2+}]_i$ following acute exposures to higher PBDE concentrations

(Dingemans *et al.*, 2010a; Dingemans et al., 2011), we quantified the effects of acute exposures to BDE-47 or BDE-49 at 20 μM on $[Ca^{2+}]_i$ (Figure 5A). Both PBDE exposures significantly increased $[Ca^{2+}]_i$ in the neuronal soma relative to vehicle controls as quantified by the maximum amplitude of transient $[Ca^{2+}]$ spikes, and the area under the curve (Figure 5B). Ca^{2+} transients localized to axonal growth cones were significantly increased by acute exposure to BDE-47 but not BDE-49 (Figure 5C).

As an alternate approach for determining whether the inhibitory effects of PBDE on axonal growth are mediated by Ca^{2+}-dependent mechanisms, we used pharmacological antagonists to investigate the role of various Ca^{2+} ion channels in PBDE neurotoxicity. Hippocampal cultures were pre-incubated 30 min prior to PBDE treatment with the L-type voltage Ca^{2+} channel blocker verapamil (30 μM), the IP_3 receptor blocker xestospongin C (1 μM) or the RyR blocker FLA365 (10 μM). These concentrations of verapamil (Keith *et al.*, 1994; Kodavanti *et al.*, 1994), xestospongin C (Gafni *et al.*, 1997; Inglefield *et al.*, 2001) and FLA365 (Chiesi *et al.*, 1988; Mack *et al.*, 1992) have previously been shown to block neuronal Ca^{2+} signaling. In the absence of PBDEs, none of these pharmacological blockers altered basal levels of axonal growth relative to vehicle controls (Figure 7A). Pretreatment of PBDE-exposed cultures with either verapamil or xestospongin did not prevent the inhibitory effects of BDE-47 and BDE-49 on axonal growth; in contrast, pretreatment with FLA365 blocked the inhibitory effects of both PBDE congeners on axonal growth (Figure 7B).

FLA365 selectively blocks RyR Ca^{2+} channels, but has been reported to also interfere with L-type Ca^{2+} channels in aterial smooth muscle cells (Ostrovskaya *et al.*, 2007). Therefore, to confirm that FLA365 antagonizes the axon inhibiting activity of PBDEs via RyR Ca^{2+} channel blockade, we determined whether siRNA knockdown of RyR phenocopies FLA365 treatment. While all three RyR isoforms are expressed in the brain, we had previously shown that RyR1 and RyR2 are predominantly expressed in primary neuron-glia co-cultures derived from P0-1 rat hippocampi (Wayman et al., 2012b). To determine whether these two RyR isoforms are

363 expressed in axonal growth cones, DIV 2 hippocampal cultures were immunostained using
364 antibodies selective for RyR1 or RyR2 and co-labeled with phalloidin to identify axonal growth
365 cones. Puncta immunoreactive for both RyR1 and RyR2 were obvious throughout the cytoplasm
366 of the axonal growth cone and even out along the tips of the phalloidin-labeled filopodia (Figure
367 8A). Expression of RyR1, RyR2 or scrambled (control) siRNA did not alter axon length in vehicle
368 control cultures. In cultures exposed to PBDEs, expression of the control siRNA did not block
369 the axon inhibitory effect of BDE-47 or BDE-49. In contrast, expression of RyR2 siRNA blocked
370 inhibitory effects of both BDE-47 and BDE-49 on axon length (Figure 8B). Expression of RyR1
371 siRNA appeared to partially block the inhibitory effect of these PBDEs on axon growth as
372 evidenced by the fact that axon lengths of PBDE-exposed neurons expressing RyR1 siRNA
373 were not significantly different from either vehicle control neurons expressing RyR1 siRNA or
374 PBDE-exposed neurons expressing control siRNA.
375
376 **Discussion (Word Limit: 1500; currently at 1489 words)**
377 Our findings support the hypothesis that PBDEs cause developmental neurotoxicity by
378 interfering with cellular and molecular mechanisms that regulate neuronal connectivity in the
379 developing brain. Specifically, our data demonstrate that BDE 47 and BDE 49 inhibit the early
380 stages of axonal growth in primary cultures of perinatal rat hippocampal neurons. These data
381 extend previous reports demonstrating that commercial PBDE mixture, DE-71, decreases
382 neurite length in primary mouse cortical cultures (Bradner *et al.*, 2013), and that BDE-47 inhibits
383 neurite outgrowth in human embryonic stem cell-derived neurons (Behl *et al.*, 2015), and
384 decreases the length of axons of motor neurons in larval zebrafish (Chen et al., 2012). In our
385 model, exposure to BDE-47 or BDE-49 significantly inhibits axonal growth at concentrations that
386 have no effect on cell viability, indicating that decreased axonal growth is not due to
387 compromised cell viability. Exposure of hippocampal cultures to the same concentration range
388 of BDE-47 or BDE-49 does not alter dendritic arborization. This suggests that PBDEs do not

389 inhibit general mechanisms of neurite outgrowth, but rather they selectively target axon-specific
390 mechanisms of growth. This observation extends previous reports demonstrating that the
391 organophosphorus pesticide chlorpyrifos (Howard *et al.*, 2005) and the NDL PCB 136 (Yang et
392 al., 2014) differentially modulate axonal *vs*. dendritic growth.

393 In contrast to axon inhibition observed when primary hippocampal neurons were exposed to
394 BDE-47 or BDE-49 during the first 48 h in culture, exposure from DIV 7-9 did not inhibit axonal
395 growth, as quantified by western blot analyses of tau 1. This raises several considerations: *(1)*
396 western blotting does not have the sensitivity to detect subtle but significant differences in
397 axonal growth; *(2)* mature neurons are more resistant to the growth inhibitory effects of PBDEs;
398 or (3) PBDEs interfere with early stages of axonal morphogenesis. Our data provide direct
399 support for the third possibility: we observed that BDE 47 and BDE 49 delay the polarization of
400 hippocampal neurons. This was evident as a significant decrease at 48 h after plating in the
401 percentage of neurons exhibiting redistribution of GAP-43 into a single neurite that was
402 noticeably longer than the remaining "minor" neurites, marking its differentiation as the neuron's
403 axon (Dotti et al., 1988; Goslin et al., 1990; Yamamoto *et al.*, 2012). This is in line with
404 previous studies demonstrating that MARCKS, an actin-binding protein enriched in axons that
405 co-distributes with GAP-43, is markedly decreased in rats exposed perinatally to BDE-71
406 (Kodavanti *et al.*, 2015; Ouimet *et al.*, 1990). Collectively, these observations support a model
407 in which PBDEs inhibit axonal growth, at least in part, by delaying neuronal polarization.

408 Neuronal polarization is controlled by $[Ca^{2+}]_i$, and Ca^{2+} ionophores completely suppress axon
409 formation in primary hippocampal neurons (Mattson *et al.*, 1990). Axonal growth requires an
410 optimal $[Ca^{2+}]_i$ in the axonal growth cone, and $[Ca^{2+}]_i$ levels on either side of this optimum inhibit
411 axonal growth (Kater and Mills, 1991). PBDEs have been shown to alter $[Ca^{2+}]_i$ in neurons via
412 mechanisms involving voltage-gated calcium channels, IP_3Rs and RyRs (Costa *et al.*, 2016;
413 Dingemans et al., 2010a; Dingemans et al., 2010b; Gassmann *et al.*, 2014; Kim et al., 2011).
414 Pharmacological block of RyRs, but not L-type calcium channels or IP_3Rs, and siRNA

knockdown of RyR2 prevents BDE-47 and BDE-49 inhibition of axonal growth, suggesting that these PBDEs inhibit axonal growth by sensitizing RyRs. Interestingly, RyR2 siRNA completely blocks, while RyR1 siRNA only partially blocks, the axon inhibitory effects of BDE 47 and BDE 49. While immunohistochemical localization data indicate that both RyR isoforms are expressed in axonal growth cones, the siRNA knockdown data suggest that RyR regulation of neuronal polarity and/or axonal growth is isoform specific.

When considered in the context of previous reports that acute exposure to BDE-47 or BDE-49 increases $[Ca^{2+}]_i$ in primary neurons (Dingemans et al., 2010a; Gassmann et al., 2014; Kim et al., 2011), our data suggest a model in which RyR sensitization by BDE-47 or BDE-49 alters local Ca^{2+} dynamics during early stages of axon development to move $[Ca^{2+}]_i$ away from the optimal levels needed for axonal specification and/or growth. However, we were not able to confirm this by documenting changes in $[Ca^{2+}]_i$ in either the soma or axonal growth cones of primary hippocampal neurons exposed to BDE-47 or BDE-49 at concentrations that inhibit axonal growth. We did observe significantly increased neuronal $[Ca^{2+}]_i$ in our model system following acute exposure to PBDE concentrations comparable to those used in the studies cited above, which were $\geq$ 10-fold higher than those that inhibit axonal growth. It is possible that the calcium fluorophore and/or imaging system we used are not sufficiently sensitive to detect spatially or temporally restricted changes in $[Ca^{2+}]_i$ (Coburn *et al.*, 2008; Dingemans et al., 2010a; Hong *et al.*, 2000; Mattson and Bruce-Keller, 1999). An alternative possibility is that Ca^{2+} is not the primary mediator of the RyR-dependent effects of PBDEs on axonal growth. Molecular effects of PBDEs other than Ca^{2+} dysregulation have been reported in experimental models of developmental neurotoxicity, including thyroid hormone dysfunction, oxidative stress and altered cholinergic, glutamatergic and GABAergic neurotransmission (Costa et al., 2014; Hendriks and Westerink, 2015). Each of these molecular actions has been implicated in axonal growth regulation (Goldberg, 2003), and RyR activity has been shown to either regulate or to be regulated by each of these molecular actions (Pessah et al., 2010). Investigating potential roles

441 for these known molecular actions in RyR-dependent inhibition of axonal growth by PBDEs is
442 the focus of ongoing studies.

443 This study yielded several unexpected findings. First, the concentration-effect relationships of
444 BDE-47 and BDE-49 on axonal growth are comparable despite significant differences in their
445 potency at the RyR (Kim et al., 2011). One possibility is that astrocytes in the coculture
446 metabolize BDE-47 to hydroxylated forms previously shown to be potent RyR sensitizers (Kim
447 et al., 2011). Whether RyR-active BDE-47 metabolites are formed in these cocultures at levels
448 sufficient to influence axonal outgrowth has yet to be determined. An alternative possibility is
449 that the RyR is not the primary molecular target but rather a downstream effector. As discussed
450 above, Ca^{2+}-independent effects of PBDEs, including thyroid hormone dysfunction, oxidative
451 stress and altered neurotransmission (Costa et al., 2014; Hendriks and Westerink, 2015), have
452 been reported to modulate RyR activity (Pessah et al., 2010). This may also explain the second
453 surprising observation, which is that PBDEs and NDL-PCBs do not phenocopy each other's
454 effects on neuronal morphogenesis. As we previously demonstrated in primary hippocampal
455 neurons, NDL PCBs enhance dendritic growth via RyR-dependent mechanisms but have no
456 effect on axonal growth (Wayman et al., 2012b; Yang et al., 2014). In contrast, using the same
457 model system, we show here that BDE-47 and BDE-49 inhibit axonal growth via RyR-
458 dependent mechanisms but have no effect on dendritic arborization. If the RyR is an
459 intermediary signaling molecule rather than the primary molecular target for PBDEs, it would not
460 be surprising that they do not phenocopy NDL PCB effects on neuronal morphogenesis.
461 Alternatively, RyR activity is regulated by numerous accessory proteins (Pessah et al., 2010),
462 and NDL PCB interactions with the RyR require the presence of the FKBP12 accessory protein
463 (Samso et al., 2009; Wong *et al.*, 1997b). While our earlier study suggests that PBDE
464 interactions with the RyR similarly require FKBP12 (Kim et al., 2011), possibly additional
465 accessory proteins are involved, and the profile of accessory proteins required for RyR
466 interactions differs between NDL PCBs and PBDEs. Since the complement of RyR accessory

proteins varies depending on the RyR isoform, and the subcellular compartment (Berridge, 2006; Pessah et al., 2010), this explanation would be consistent with our observation that both RyR1 and RyR2 activity are required for the dendrite promoting activity of NDL PCBs (Wayman et al., 2012b), while only RyR2 is required for the axon inhibiting effects of PBDEs. A related possibility derives from observations that the kinetics of changes in $[Ca^{2+}]_i$ influence the profile of activated downstream effectors (Berridge, 2006; Mattson, 1992). If the kinetics of PBDE effects on RyR gating are different than those of NDL PCBs, they could activate unique downstream effectors, resulting in differential effects on axons *vs*. dendrites. Future mechanistic studies are warranted to distinguish the relative contributions of these possibilities to the distinct toxicological profiles of PBDEs *vs*. NDL PCBs.

The human relevance of these *in vitro* mechanistic studies is suggested by the observation that the effects BDE-47 and BDE-49 were observed at concentrations as low as 0.2 nM, which are well within the range of PBDE plasma concentrations detected in highly exposed human populations (Eskenazi et al., 2013; Eskenazi *et al.*, 2011; Hertz-Picciotto *et al.*, 2011). Whether PBDE effects on axon growth contribute to neurobehavioral deficits associated with developmental exposure remains to be determined. However, evidence that spatiotemporal patterns in axonal growth can cause persistent changes in brain patterning and connectivity (Berger-Sweeney and Hohmann, 1997; Cremer *et al.*, 1997; Maier *et al.*, 1999), and are linked to neurodevelopmental disorders (Copf, 2016; Robichaux and Cowan, 2014), gives credence to the possibility that inhibition of axonal growth is important in PBDE developmental neurotoxicity.

Supplementary Data Description

Supplemental files provide information regarding the synthesis and purity of FLA 365 (File S1), representative phase contrast photomicrographs of cultures used for these studies (File S2), and Ca^{2+} imaging data from cultures exposed acutely to BDE levels shown to inhibit axonal growth (File S3).

Funding Information

This work was supported by the National Institute of Environmental Health Sciences [grant numbers R01 ES014901, P01 ES011269, P42 ES04699, U54 HD079125, F32 ES024676 to KMS, T32-MH073124 (postdoctoral fellowship) to KMS, and T32 ES007059 (predoctoral fellowship) to HC], the United States Environmental Protection Agency [grant numbers RD835550 and R83543201] and the J.B. Johnson Foundation [unrestricted gift to PJL]. The sponsors were not involved in the study design, the collection, analysis, and interpretation of data, in the writing of the report or in the decision to submit the paper for publication.

Acknowledgments

The authors thank Dr. Kimberly P. Keil (UC Davis) and Dr. Keri A. Hayakawa (UC Davis) for providing helpful feedback on early drafts of the manuscript.

References

Adasme T, Haeger P, Paula-Lima AC, Espinoza I, Casas-Alarcon MM, Carrasco MA, and Hidalgo C (2011). Involvement of ryanodine receptors in neurotrophin-induced hippocampal synaptic plasticity and spatial memory formation. *Proc Natl Acad Sci U S A* **108**(7), 3029-34.

Arie Y, Iketani M, Takamatsu K, Mikoshiba K, Goshima Y, and Takei K (2009). Developmental changes in the regulation of calcium-dependent neurite outgrowth. *Biochem Biophys Res Commun* **379**(1), 11-5.

Behl M, Hsieh JH, Shafer TJ, Mundy WR, Rice JR, Boyd WA, Freedman JH, Hunter ES, 3rd, Jarema KA, Padilla S, and Tice RR (2015). Use of alternative assays to identify and prioritize organophosphorus flame retardants for potential developmental and neurotoxicity. *Neurotoxicol Teratol* **52**(Pt B), 181-93.

Berger-Sweeney J, and Hohmann CF (1997). Behavioral consequences of abnormal cortical development: insights into developmental disabilities. *Behav Brain Res* **86**(2), 121-42.

Berridge MJ (2006). Calcium microdomains: organization and function. *Cell Calcium* **40**(5-6), 405-12.

Bradner JM, Suragh TA, and Caudle WM (2013). Alterations to the circuitry of the frontal cortex following exposure to the polybrominated diphenyl ether mixture, DE-71. *Toxicology* **312**, 48-55.

Chandrasekaran V, Lea C, Sosa JC, Higgins D, and Lein PJ (2015). Reactive oxygen species are involved in BMP-induced dendritic growth in cultured rat sympathetic neurons. *Mol Cell Neurosci* **67**, 116-25.

Chao HR, Tsou TC, Huang HL, and Chang-Chien GP (2011). Levels of breast milk PBDEs from southern Taiwan and their potential impact on neurodevelopment. *Pediatr Res* **70**(6), 596-600.

Chen X, Huang C, Wang X, Chen J, Bai C, Chen Y, Chen X, Dong Q, and Yang D (2012). BDE-47 disrupts axonal growth and motor behavior in developing zebrafish. *Aquat Toxicol* **120-121**, 35-44.

Chiesi M, Schwaller R, and Calviello G (1988). Inhibition of rapid Ca-release from isolated skeletal and cardiac sarcoplasmic reticulum (SR) membranes. *Biochem Biophys Res Commun* **154**(1), 1-8.
Coburn CG, Curras-Collazo MC, and Kodavanti PR (2008). In vitro effects of environmentally relevant polybrominated diphenyl ether (PBDE) congeners on calcium buffering mechanisms in rat brain. *Neurochem Res* **33**(2), 355-64.
Copf T (2016). Impairments in dendrite morphogenesis as etiology for neurodevelopmental disorders and implications for therapeutic treatments. *Neurosci Biobehav Rev* **68**, 946-978.
Costa LG, de Laat R, Tagliaferri S, and Pellacani C (2014). A mechanistic view of polybrominated diphenyl ether (PBDE) developmental neurotoxicity. *Toxicol Lett* **230**(2), 282-94.
Costa LG, Tagliaferri S, Roque PJ, and Pellacani C (2016). Role of glutamate receptors in tetrabrominated diphenyl ether (BDE-47) neurotoxicity in mouse cerebellar granule neurons. *Toxicol Lett* **241**, 159-66.
Cremer H, Chazal G, Goridis C, and Represa A (1997). NCAM is essential for axonal growth and fasciculation in the hippocampus. *Mol Cell Neurosci* **8**(5), 323-35.
Dingemans MM, Heusinkveld HJ, Bergman A, van den Berg M, and Westerink RH (2010a). Bromination pattern of hydroxylated metabolites of BDE-47 affects their potency to release calcium from intracellular stores in PC12 cells. *Environ Health Perspect* **118**(4), 519-25.
Dingemans MM, van den Berg M, Bergman A, and Westerink RH (2010b). Calcium-related processes involved in the inhibition of depolarization-evoked calcium increase by hydroxylated PBDEs in PC12 cells. *Toxicol Sci* **114**(2), 302-9.
Dingemans MM, van den Berg M, and Westerink RH (2011). Neurotoxicity of brominated flame retardants: (in)direct effects of parent and hydroxylated polybrominated diphenyl ethers on the (developing) nervous system. *Environ Health Perspect* **119**(7), 900-7.
Dotti CG, Sullivan CA, and Banker GA (1988). The establishment of polarity by hippocampal neurons in culture. *J Neurosci* **8**(4), 1454-68.
EFSA (2011). Scientific opinion on polybrominated diphenyl ethers (PBDEs) in food. *EFSA J.* **9**(2156), 274.
Eskenazi B, Chevrier J, Rauch SA, Kogut K, Harley KG, Johnson C, Trujillo C, Sjodin A, and Bradman A (2013). In utero and childhood polybrominated diphenyl ether (PBDE) exposures and neurodevelopment in the CHAMACOS study. *Environ Health Perspect* **121**(2), 257-62.
Eskenazi B, Fenster L, Castorina R, Marks AR, Sjodin A, Rosas LG, Holland N, Guerra AG, Lopez-Carillo L, and Bradman A (2011). A comparison of PBDE serum concentrations in Mexican and Mexican-American children living in California. *Environ Health Perspect* **119**(10), 1442-8.
Florvall L, Ask AL, Ogren SO, and Ross SB (1977). Selective monoamine oxidase inhibitors. *J Med Chem* **21**, 56-63.
Gafni J, Munsch JA, Lam TH, Catlin MC, Costa LG, Molinski TF, and Pessah IN (1997). Xestospongins: potent membrane permeable blockers of the inositol 1,4,5-trisphosphate receptor. *Neuron* **19**(3), 723-33.
Gascon M, Fort M, Martinez D, Carsin AE, Forns J, Grimalt JO, Santa Marina L, Lertxundi N, Sunyer J, and Vrijheid M (2012). Polybrominated diphenyl ethers (PBDEs) in breast milk and neuropsychological development in infants. *Environ Health Perspect* **120**(12), 1760-5.
Gassmann K, Schreiber T, Dingemans MM, Krause G, Roderigo C, Giersiefer S, Schuwald J, Moors M, Unfried K, Bergman A, Westerink RH, Rose CR, and Fritsche E (2014). BDE-47 and 6-OH-BDE-47 modulate calcium homeostasis in primary fetal human neural progenitor cells via ryanodine receptor-independent mechanisms. *Arch Toxicol* **88**(8), 1537-48.
Goldberg JL (2003). How does an axon grow? *Genes Dev* **17**(8), 941-58.
Gomez TM, Snow DM, and Letourneau PC (1995). Characterization of spontaneous calcium transients in nerve growth cones and their effect on growth cone migration. *Neuron* **14**(6), 1233-46.

Goslin K, and Banker G (1990). Rapid changes in the distribution of GAP-43 correlate with the expression of neuronal polarity during normal development and under experimental conditions. *J Cell Biol* **110**(4), 1319-31.

Goslin K, Schreyer DJ, Skene JH, and Banker G (1990). Changes in the distribution of GAP-43 during the development of neuronal polarity. *J Neurosci* **10**(2), 588-602.

Harrill JA, Freudenrich TM, Robinette BL, and Mundy WR (2011). Comparative sensitivity of human and rat neural cultures to chemical-induced inhibition of neurite outgrowth. *Toxicol Appl Pharmacol* **256**(3), 268-80.

Harrill JA, Robinette BL, Freudenrich T, and Mundy WR (2013). Use of high content image analyses to detect chemical-mediated effects on neurite sub-populations in primary rat cortical neurons. *Neurotoxicology* **34**, 61-73.

Hayashi K, Kawai-Hirai R, Ishikawa K, and Takata K (2002). Reversal of neuronal polarity characterized by conversion of dendrites into axons in neonatal rat cortical neurons in vitro. *Neuroscience* **110**(1), 7-17.

Hendriks HS, and Westerink RH (2015). Neurotoxicity and risk assessment of brominated and alternative flame retardants. *Neurotoxicol Teratol* **52**(Pt B), 248-69.

Herbstman JB, Sjodin A, Kurzon M, Lederman SA, Jones RS, Rauh V, Needham LL, Tang D, Niedzwiecki M, Wang RY, and Perera F (2010). Prenatal exposure to PBDEs and neurodevelopment. *Environ Health Perspect* **118**(5), 712-9.

Hertle DN, and Yeckel MF (2007). Distribution of inositol-1,4,5-trisphosphate receptor isotypes and ryanodine receptor isotypes during maturation of the rat hippocampus. *Neuroscience* **150**(3), 625-38.

Hertz-Picciotto I, Bergman A, Fangstrom B, Rose M, Krakowiak P, Pessah I, Hansen R, and Bennett DH (2011). Polybrominated diphenyl ethers in relation to autism and developmental delay: a case-control study. *Environ Health* **10**(1), 1.

Hoffman K, Adgent M, Goldman BD, Sjodin A, and Daniels JL (2012). Lactational exposure to polybrominated diphenyl ethers and its relation to social and emotional development among toddlers. *Environ Health Perspect* **120**(10), 1438-42.

Hong K, Nishiyama M, Henley J, Tessier-Lavigne M, and Poo M (2000). Calcium signalling in the guidance of nerve growth by netrin-1. *Nature* **403**(6765), 93-8.

Howard AS, Bucelli R, Jett DA, Bruun D, Yang D, and Lein PJ (2005). Chlorpyrifos exerts opposing effects on axonal and dendritic growth in primary neuronal cultures. *Toxicol Appl Pharmacol* **207**(2), 112-24.

Inglefield JR, Mundy WR, and Shafer TJ (2001). Inositol 1,4,5-triphosphate receptor-sensitive Ca(2+) release, store-operated Ca(2+) entry, and cAMP responsive element binding protein phosphorylation in developing cortical cells following exposure to polychlorinated biphenyls. *J Pharmacol Exp Ther* **297**(2), 762-73.

Jacques-Fricke BT, Seow Y, Gottlieb PA, Sachs F, and Gomez TM (2006). Ca2+ influx through mechanosensitive channels inhibits neurite outgrowth in opposition to other influx pathways and release from intracellular stores. *J Neurosci* **26**(21), 5656-64.

Kapfhammer JP (2004). Cellular and molecular control of dendritic growth and development of cerebellar Purkinje cells. *Prog Histochem Cytochem* **39**(3), 131-82.

Kater SB, and Mills LR (1991). Regulation of growth cone behavior by calcium. *J Neurosci* **11**(4), 891-9.

Keith RA, Mangano TJ, DeFeo PA, Ernst GE, and Warawa EJ (1994). Differential inhibition of neuronal calcium entry and [3H]-D-aspartate release by the quaternary derivatives of verapamil and emopamil. *Br J Pharmacol* **113**(2), 379-84.

Kim KH, Bose DD, Ghogha A, Riehl J, Zhang R, Barnhart CD, Lein PJ, and Pessah IN (2011). Para- and ortho-substitutions are key determinants of polybrominated diphenyl ether activity toward ryanodine receptors and neurotoxicity. *Environ Health Perspect* **119**(4), 519-26.

Kodavanti PR, and Curras-Collazo MC (2010). Neuroendocrine actions of organohalogens: thyroid hormones, arginine vasopressin, and neuroplasticity. *Front Neuroendocrinol* **31**(4), 479-96.

621 Kodavanti PR, Royland JE, Osorio C, Winnik WM, Ortiz P, Lei L, Ramabhadran R, and Alzate O (2015).
622 Developmental exposure to a commercial PBDE mixture: effects on protein networks in the cerebellum
623 and hippocampus of rats. *Environ Health Perspect* **123**(5), 428-36.
624 Kodavanti PR, Shafer TJ, Ward TR, Mundy WR, Freudenrich T, Harry GJ, and Tilson HA (1994). Differential
625 effects of polychlorinated biphenyl congeners on phosphoinositide hydrolysis and protein kinase C
626 translocation in rat cerebellar granule cells. *Brain Res* **662**(1-2), 75-82.
627 Lein PJ, Banker GA, and Higgins D (1992). Laminin selectively enhances axonal growth and accelerates
628 the development of polarity by hippocampal neurons in culture. *Brain Res Dev Brain Res* **69**(2), 191-7.
629 Lobner D (2000). Comparison of the LDH and MTT assays for quantifying cell death: validity for neuronal
630 apoptosis? *J Neurosci Methods* **96**(2), 147-52.
631 Lohmann C, and Wong RO (2005). Regulation of dendritic growth and plasticity by local and global
632 calcium dynamics. *Cell Calcium* **37**(5), 403-9.
633 Lunder S, Hovander L, Athanassiadis I, and Bergman A (2010). Significantly higher polybrominated
634 diphenyl ether levels in young U.S. children than in their mothers. *Environ Sci Technol* **44**(13), 5256-62.
635 Mack WM, Zimanyi I, and Pessah IN (1992). Discrimination of multiple binding sites for antagonists of
636 the calcium release channel complex of skeletal and cardiac sarcoplasmic reticulum. *J Pharmacol Exp*
637 *Ther* **262**(3), 1028-37.
638 Maier DL, Mani S, Donovan SL, Soppet D, Tessarollo L, McCasland JS, and Meiri KF (1999). Disrupted
639 cortical map and absence of cortical barrels in growth-associated protein (GAP)-43 knockout mice. *Proc*
640 *Natl Acad Sci U S A* **96**(16), 9397-402.
641 Mattson MP (1992). Calcium as sculptor and destroyer of neural circuitry. *Exp Gerontol* **27**(1), 29-49.
642 Mattson MP, and Bruce-Keller AJ (1999). Compartmentalization of signaling in neurons: evolution and
643 deployment. *J Neurosci Res* **58**(1), 2-9.
644 Mattson MP, Murain M, and Guthrie PB (1990). Localized calcium influx orients axon formation in
645 embryonic hippocampal pyramidal neurons. *Brain Res Dev Brain Res* **52**(1-2), 201-9.
646 Meijering E, Jacob M, Sarria JC, Steiner P, Hirling H, and Unser M (2004). Design and validation of a tool
647 for neurite tracing and analysis in fluorescence microscopy images. *Cytometry A* **58**(2), 167-76.
648 Miller MF, Chernyak SM, Batterman S, and Loch-Caruso R (2009). Polybrominated diphenyl ethers in
649 human gestational membranes from women in southeast Michigan. *Environ Sci Technol* **43**(9), 3042-6.
650 Mosmann T (1983). Rapid colorimetric assay for cellular growth and survival: application to proliferation
651 and cytotoxicity assays. *J Immunol Methods* **65**(1-2), 55-63.
652 Ohashi R, Sakata S, Naito A, Hirashima N, and Tanaka M (2014). Dendritic differentiation of cerebellar
653 Purkinje cells is promoted by ryanodine receptors expressed by Purkinje and granule cells. *Dev Neurobiol*
654 **74**(4), 467-80.
655 Ooashi N, Futatsugi A, Yoshihara F, Mikoshiba K, and Kamiguchi H (2005). Cell adhesion molecules
656 regulate Ca2+-mediated steering of growth cones via cyclic AMP and ryanodine receptor type 3. *J Cell*
657 *Biol* **170**(7), 1159-67.
658 Ostrovskaya O, Goyal R, Osman N, McAllister CE, Pessah IN, Hume JR, and Wilson SM (2007). Inhibition
659 of ryanodine receptors by 4-(2-aminopropyl)-3,5-dichloro-N,N-dimethylaniline (FLA 365) in canine
660 pulmonary arterial smooth muscle cells. *J Pharmacol Exp Ther* **323**(1), 381-90.
661 Ouimet CC, Wang JK, Walaas SI, Albert KA, and Greengard P (1990). Localization of the MARCKS (87 kDa)
662 protein, a major specific substrate for protein kinase C, in rat brain. *J Neurosci* **10**(5), 1683-98.
663 Pessah IN, Cherednichenko G, and Lein PJ (2010). Minding the calcium store: Ryanodine receptor
664 activation as a convergent mechanism of PCB toxicity. *Pharmacol Ther* **125**(2), 260-85.
665 Robichaux MA, and Cowan CW (2014). Signaling mechanisms of axon guidance and early
666 synaptogenesis. *Curr Top Behav Neurosci* **16**, 19-48.

Roze E, Meijer L, Bakker A, Van Braeckel KN, Sauer PJ, and Bos AF (2009). Prenatal exposure to organohalogens, including brominated flame retardants, influences motor, cognitive, and behavioral performance at school age. *Environ Health Perspect* **117**(12), 1953-8.
Samso M, Feng W, Pessah IN, and Allen PD (2009). Coordinated movement of cytoplasmic and transmembrane domains of RyR1 upon gating. *PLoS Biol* **7**(4), e85.
Seymour-Laurent KJ, and Barish ME (1995). Inositol 1,4,5-trisphosphate and ryanodine receptor distributions and patterns of acetylcholine- and caffeine-induced calcium release in cultured mouse hippocampal neurons. *J Neurosci* **15**(4), 2592-608.
She J, Holden A, Sharp M, Tanner M, Williams-Derry C, and Hooper K (2007). Polybrominated diphenyl ethers (PBDEs) and polychlorinated biphenyls (PCBs) in breast milk from the Pacific Northwest. *Chemosphere* **67**(9), S307-17.
Shy CG, Huang HL, Chang-Chien GP, Chao HR, and Tsou TC (2011). Neurodevelopment of infants with prenatal exposure to polybrominated diphenyl ethers. *Bull Environ Contam Toxicol* **87**(6), 643-8.
Stamou M, Streifel KM, Goines PE, and Lein PJ (2013). Neuronal connectivity as a convergent target of gene x environment interactions that confer risk for Autism Spectrum Disorders. *Neurotoxicol Teratol* **36**, 3-16.
Toms LM, Sjodin A, Harden F, Hobson P, Jones R, Edenfield E, and Mueller JF (2009). Serum polybrominated diphenyl ether (PBDE) levels are higher in children (2-5 years of age) than in infants and adults. *Environ Health Perspect* **117**(9), 1461-5.
USEPA (2010). An Exposure Assessment of Polybrominated Diphenyl Ethers. 378.
Valnegri P, Puram SV, and Bonni A (2015). Regulation of dendrite morphogenesis by extrinsic cues. *Trends Neurosci* **38**(7), 439-47.
Vaughan PJ, Pike CJ, Cotman CW, and Cunningham DD (1995). Thrombin receptor activation protects neurons and astrocytes from cell death produced by environmental insults. *J Neurosci* **15**(7 Pt 2), 5389-401.
Wayman GA, Bose DD, Yang D, Lesiak A, Bruun D, Impey S, Ledoux V, Pessah IN, and Lein PJ (2012a). PCB-95 modulates the calcium-dependent signaling pathway responsible for activity-dependent dendritic growth. *Environ Health Perspect* **120**(7), 1003-9.
Wayman GA, Impey S, Marks D, Saneyoshi T, Grant WF, Derkach V, and Soderling TR (2006). Activity-dependent dendritic arborization mediated by CaM-kinase I activation and enhanced CREB-dependent transcription of Wnt-2. *Neuron* **50**(6), 897-909.
Wayman GA, Yang D, Bose DD, Lesiak A, Ledoux V, Bruun D, Pessah IN, and Lein PJ (2012b). PCB-95 promotes dendritic growth via ryanodine receptor-dependent mechanisms. *Environ Health Perspect* **120**(7), 997-1002.
Welshhans K, and Rehder V (2007). Nitric oxide regulates growth cone filopodial dynamics via ryanodine receptor-mediated calcium release. *Eur J Neurosci* **26**(6), 1537-47.
Wiggin GR, Fawcett JP, and Pawson T (2005). Polarity proteins in axon specification and synaptogenesis. *Dev Cell* **8**(6), 803-16.
Wong PW, Brackney WR, and Pessah IN (1997a). Ortho-substituted polychlorinated biphenyls alter microsomal calcium transport by direct interaction with ryanodine receptors of mammalian brain. *J Biol Chem* **272**(24), 15145-53.
Wong PW, Joy RM, Albertson TE, Schantz SL, and Pessah IN (1997b). Ortho-substituted 2,2',3,5',6-pentachlorobiphenyl (PCB 95) alters rat hippocampal ryanodine receptors and neuroplasticity in vitro: evidence for altered hippocampal function. *Neurotoxicology* **18**(2), 443-56.
Wong PW, and Pessah IN (1996). Ortho-substituted polychlorinated biphenyls alter calcium regulation by a ryanodine receptor-mediated mechanism: structural specificity toward skeletal- and cardiac-type microsomal calcium release channels. *Mol Pharmacol* **49**(4), 740-51.

Yamamoto H, Demura T, Morita M, Banker GA, Tanii T, and Nakamura S (2012). Differential neurite outgrowth is required for axon specification by cultured hippocampal neurons. *J Neurochem* **123**(6), 904-10.
Yang D, Kania-Korwel I, Ghogha A, Chen H, Stamou M, Bose DD, Pessah IN, Lehmler HJ, and Lein PJ (2014). PCB 136 atropselectively alters morphometric and functional parameters of neuronal connectivity in cultured rat hippocampal neurons via ryanodine receptor-dependent mechanisms. *Toxicol Sci* **138**(2), 379-92.
Yang D, Kim KH, Phimister A, Bachstetter AD, Ward TR, Stackman RW, Mervis RF, Wisniewski AB, Klein SL, Kodavanti PR, Anderson KA, Wayman G, Pessah IN, and Lein PJ (2009). Developmental exposure to polychlorinated biphenyls interferes with experience-dependent dendritic plasticity and ryanodine receptor expression in weanling rats. *Environ Health Perspect* **117**(3), 426-35.
Zheng JQ, and Poo MM (2007). Calcium signaling in neuronal motility. *Annu Rev Cell Dev Biol* **23**, 375-404.

Figure Legends

Figure 1. BDE-47 and BDE-49 do not alter dendritic growth in cultured hippocampal neurons. Cells dissociated from postnatal day 1 (P1) rat hippocampi were transfected with MAP2B-eGFP at day *in vitro* (DIV) 6. On DIV 7, cultures were exposed to vehicle (DMSO diluted 1:1000) or varying concentrations of BDE-47 or BDE-49 for 48 h. (A) Representative photomicrographs of DIV 9 neurons expressing MAP2B-eGFP following exposure to vehicle, BDE-47 (200 nM) or BDE-49 (200 nM). PCB 95 (200 nM) was added to a subset of cultures as a positive control. (B) Quantification of dendritic length in GFP+ neurons. Data from one experiment presented as the mean ± SE (n=30-40 neurons per condition from 3 cultures in one independent dissection). Experiments were repeated in 3 independent dissections with comparable results from each experiment. *$p<0.05$ relative to vehicle control. Scale bar = 25 μm.

Figure 2. BDE-47 and BDE-49 reduce axon length in cultured hippocampal neurons. Cells dissociated from P1 rat hippocampi were exposed to vehicle or varying concentrations of BDE-47 or BDE-49 beginning 3 h after plating. After a 48 h exposure, neurons (DIV 2) were fixed and immunostained for Tau-1. (A) Representative photomicrographs of DIV 2 hippocampal neurons

exposed to vehicle, BDE-47 (200 nM) or BDE-49 (200 nM). (B) Quantification of axon length in Tau-1 immunopositive cells. Data presented as the mean ± SE (n=70-90 neurons from 3 independent dissections in all groups except for the 20 pM group in which n=40 neurons from 3 independent dissections). **p<0.01, ***p<0.001 relative to vehicle control. Scale bar = 10 μm.

Figure 3. BDE-47 and BDE-49 are not cytotoxic at concentrations that decrease axon length. LDH release into the media (A) and live-dead staining using calcein AM and propidium iodide (B) were used to assess cell viability in dissociated hippocampal cultures on DIV 2 following a 48 h exposure to vehicle or varying concentrations of BDE 47 or BDE 49. 0.1% Triton X-100 was used as a positive control. Data presented as mean ± SE (n=3 independent dissections). *p<0.05, ***p<0.0001 relative to vehicle control.

Figure 4. BDE-47 and BDE-49 do not decrease tau-1 expression in mature cultures. At DIV 5, hippocampal neurons were treated with BDE-47 (A) or BDE-49 (B) for 48 h. Sodium orthovanadate (30 μM) was used as a positive control (Harrill *et al.*, 2011). At the end of the exposure, cells were lysed for western blotting and probed with antibodies specific for tau-1 (axonal cytoskeletal protein) and GAPDH (loading control) as shown in representative western blots (top panels). Bar graphs (bottom panel) represent densitometric data. Densitometric values of tau-1 immunopositive bands were normalized to densitometric values for GAPDH immunopositive bands within the same sample. Data presented as mean ± SE (n=4 independent dissections). ***p<0.001 relative to vehicle control.

Figure 5. BDE-47 and BDE-49 delay the development of polarity in hippocampal neurons. Polarity was quantified in dissociated hippocampal cell cultures based on the subcellular distribution of GAP-43 immunoreactivity and morphometric criteria. (A) Representative photomicrographs of hippocampal neurons at different stages of polarization. (B) Ontogeny of

polarity in hippocampal cultures grown under the culture conditions used in this study. (C) Percent of polarized (Stage 3) neurons at DIV 2 following a 48 h exposure to vehicle, BDE-47 (200 nM) or BDE-49 (200 nM). Data presented as mean ± SE (n=9 coverslips collected from 3 independent dissections, 70-150 neurons each coverslip). *p<0.05 relative to vehicle control. Scale bar = 10 μm.

Figure 6. Acute exposure to BDE-47 and BDE-49 increases $[Ca^{2+}]_i$ in cultured hippocampal neurons. DIV 2 hippocampal cultures were loaded with Fluo-4AM (4 μM) and imaged for 26 min to quantify spontaneous calcium transients. (A) Combined traces of neuronal responses to vehicle (n=69), 20 μM BDE-47 (n=57) or 20 μM BDE-49 (n=49). Arrow indicates when PBDE or vehicle were added to the culture, typically after 5 min of baseline recording. Bar graphs at the right summarize the maximal amplitude of the Ca^{2+} signal normalized to baseline (F/Fo) and the area under the curve (AUC) of signal above the baseline amplitude in the neuronal cell soma (B) and growth cones (C). Data presented as mean ± SE (n=4 independent dissections). *p<0.05, ***p<0.0001 relative to vehicle control.

Figure 7. Pharmacological block of RyR Ca^{2+} channels prevents the inhibitory effects of BDE-47 or BDE-49 on axon length. Dissociated hippocampal cell cultures were pre-treated with the L-type Ca^{2+} channel blocker verapamil (30 μM), the IP_3 receptor blocker xestospongin C (1 μM) or the RyR blocker FLA365 (10 μM) 30 min prior to addition of vehicle, BDE-47 (200 nM) or BDE-49 (200 nM). After 48 h, cultures were fixed and immunostained for Tau-1. Axon length was quantified in cultures treated with pharmacological inhibitors in the absence (A) or presence (B) of BDEs. Data presented as the mean ± SE (n=30-60 neurons each condition from 3 cultures derived from a single dissection). This experiment was repeated in culture derived from 3 independent dissections with comparable results. *p<0.05 relative to vehicle control, #p<0.05 relative to BDE-matched cultures not treated with a pharmacological inhibitor.

Figure 8. BDE-47 and BDE-49 reduce axon length via RyR2-dependent mechanism(s). (A) Representative photomicrographs of axonal growth cones in DIV 2 hippocampal cultures co-labeled with fluorescently tagged phalloidin (green) and antibody selective for RyR1 (red, left) or RyR2 (red, right). (B) Quantitative analyses of axonal length in Cy5 positive neurons. Dissociated hippocampal cells were electroporated with Cy5-labeled scrambled (control), RYR1 or RYR2 siRNA prior to plating. Data presented as the mean ± SE (n=90 neurons collected from 3 independent dissections). *p<0.05 relative to vehicle control, #p<0.05 relative to cultures transfected with control siRNA and exposed to the same BDE. Scale bar = 5 μm.

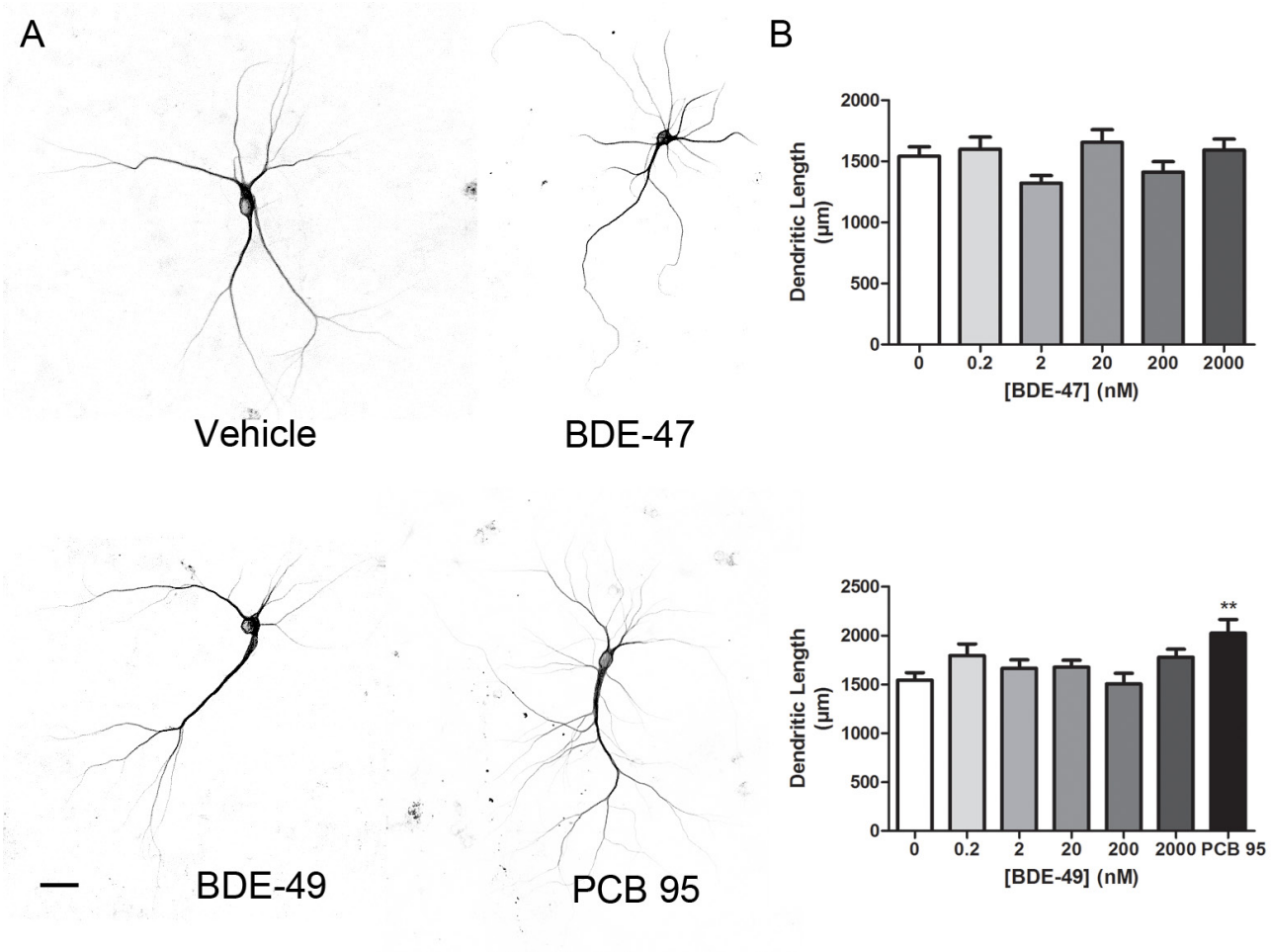

Figure 1.

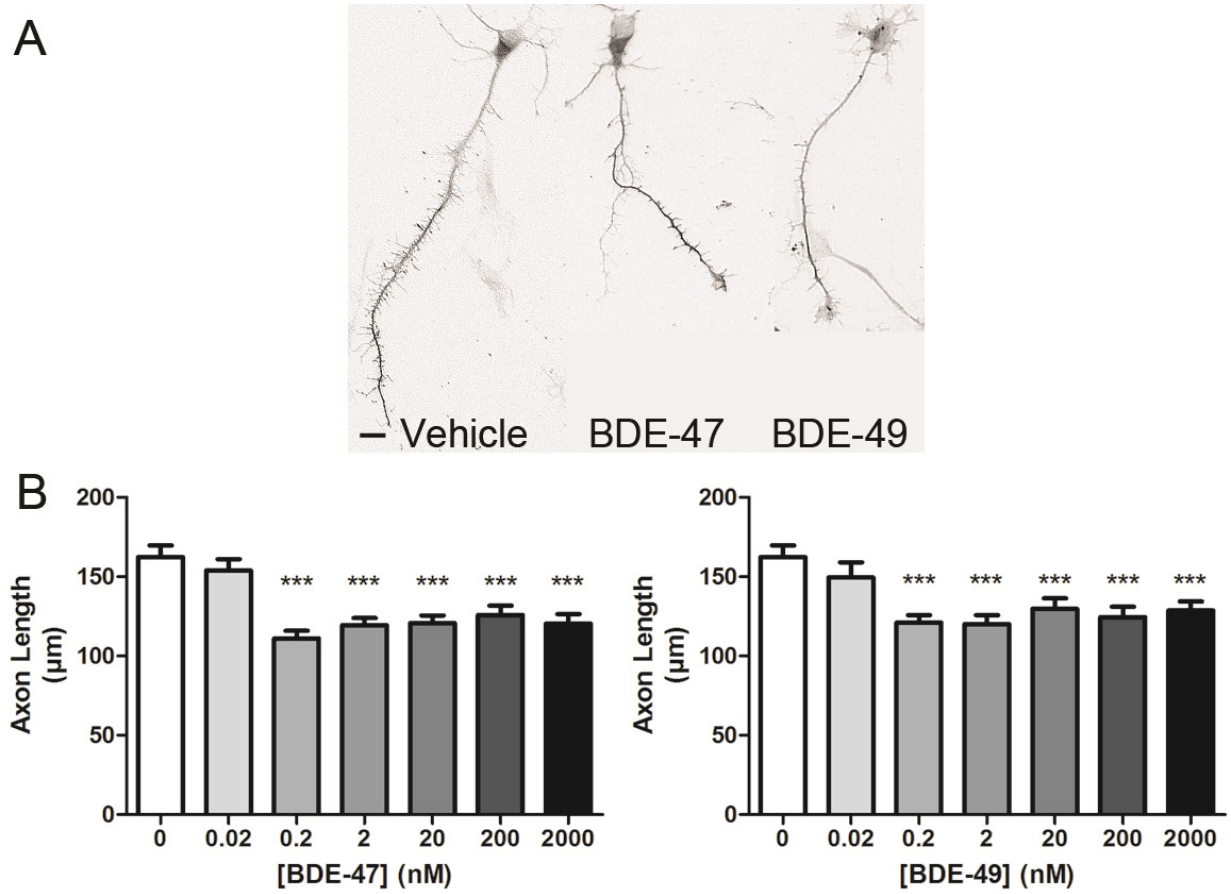
A
Vehicle
BDE-47
BDE-49
B
Axon Length (µm)
200
150
100
50
0
***
0
0.02
0.2
2
20
200
2000
[BDE-47] (nM)
[BDE-49] (nM)

Figure 2.

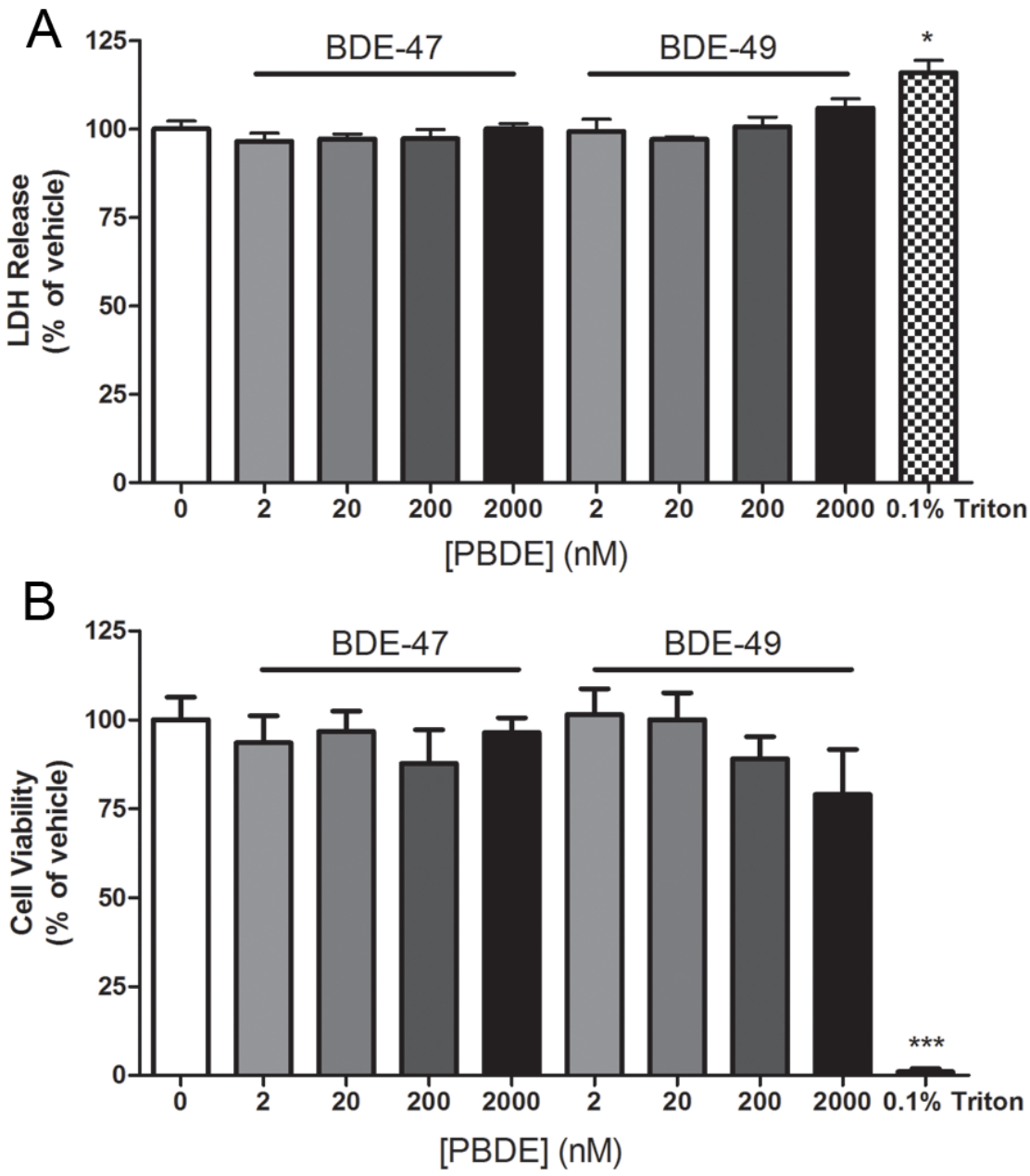
A
BDE-47
BDE-49
*
LDH Release
(% of vehicle)
125
100
75
50
25
0
0
2
20
200
2000
2
20
200
2000
0.1% Triton
[PBDE] (nM)
B
BDE-47
BDE-49
Cell Viability
(% of vehicle)
125
100
75
50
25
0
***
0
2
20
200
2000
2
20
200
2000
0.1% Triton
[PBDE] (nM)

Figure 3.

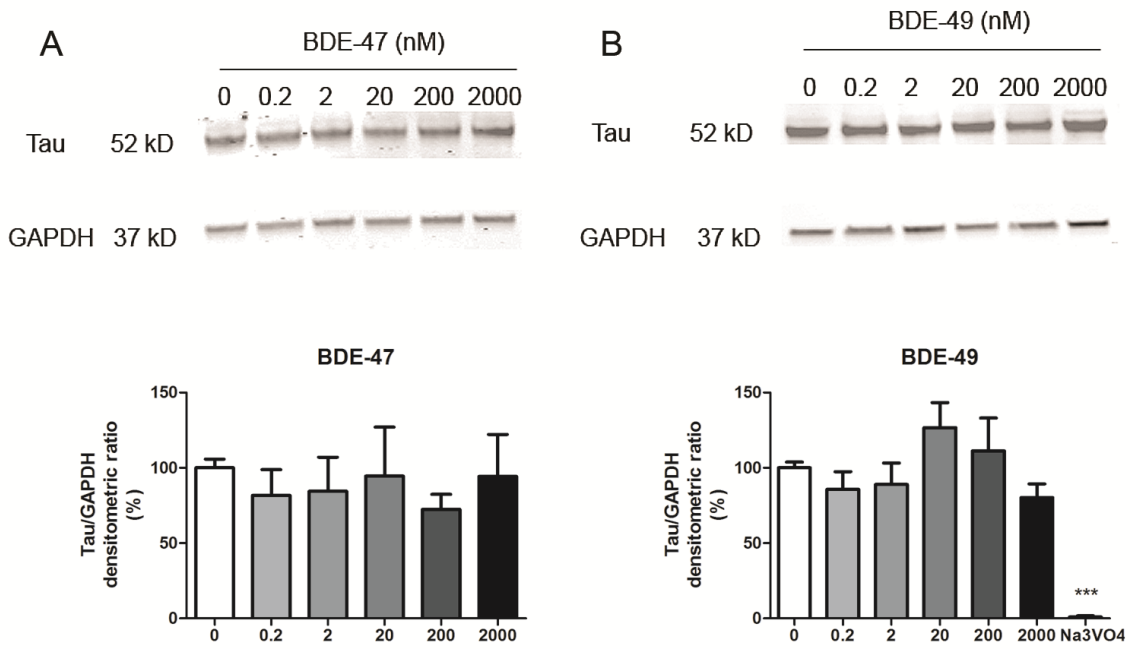

812

813 **Figure 4.**

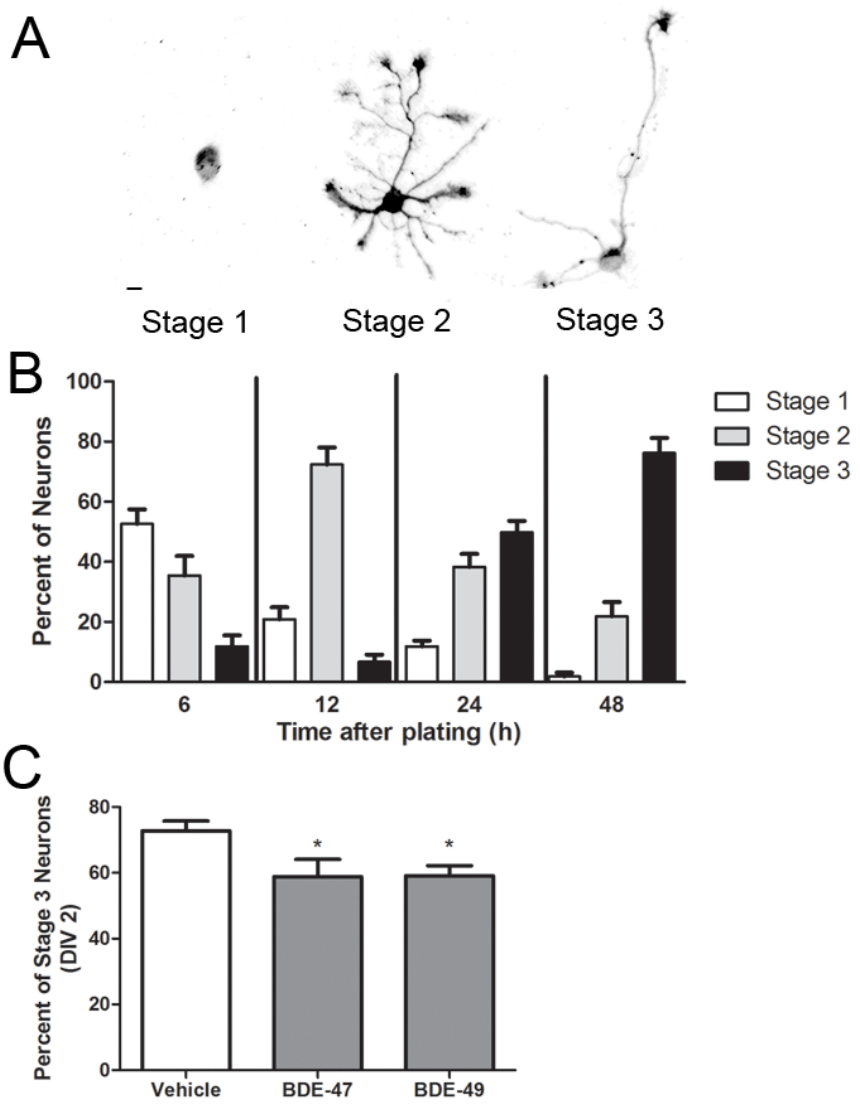
A
Stage 1
Stage 2
Stage 3
B
Percent of Neurons
100
80
60
40
20
0
6
12
24
48
Time after plating (h)
Stage 1
Stage 2
Stage 3
C
Percent of Stage 3 Neurons (DIV 2)
80
60
40
20
0
*
*
Vehicle
BDE-47
BDE-49

Figure 5.

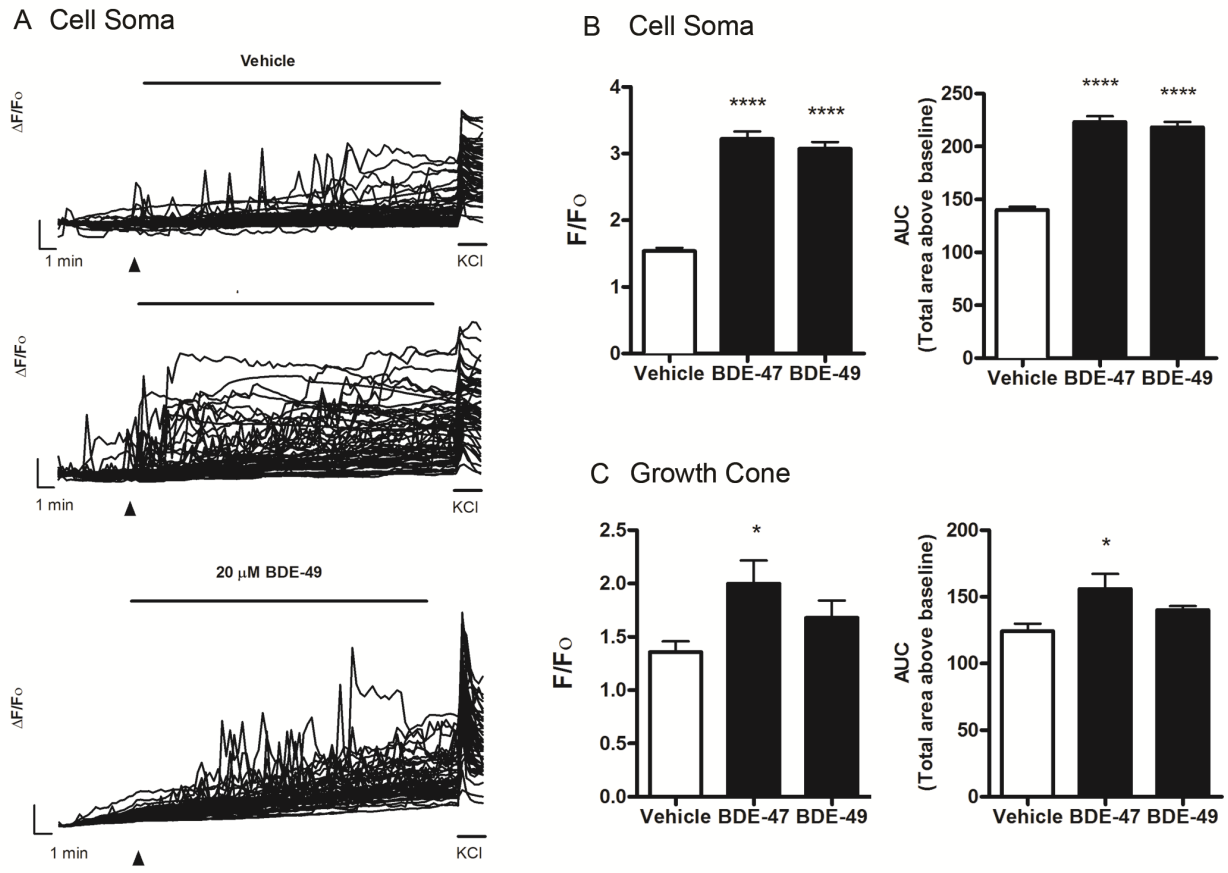

816

817 **Figure 6.**

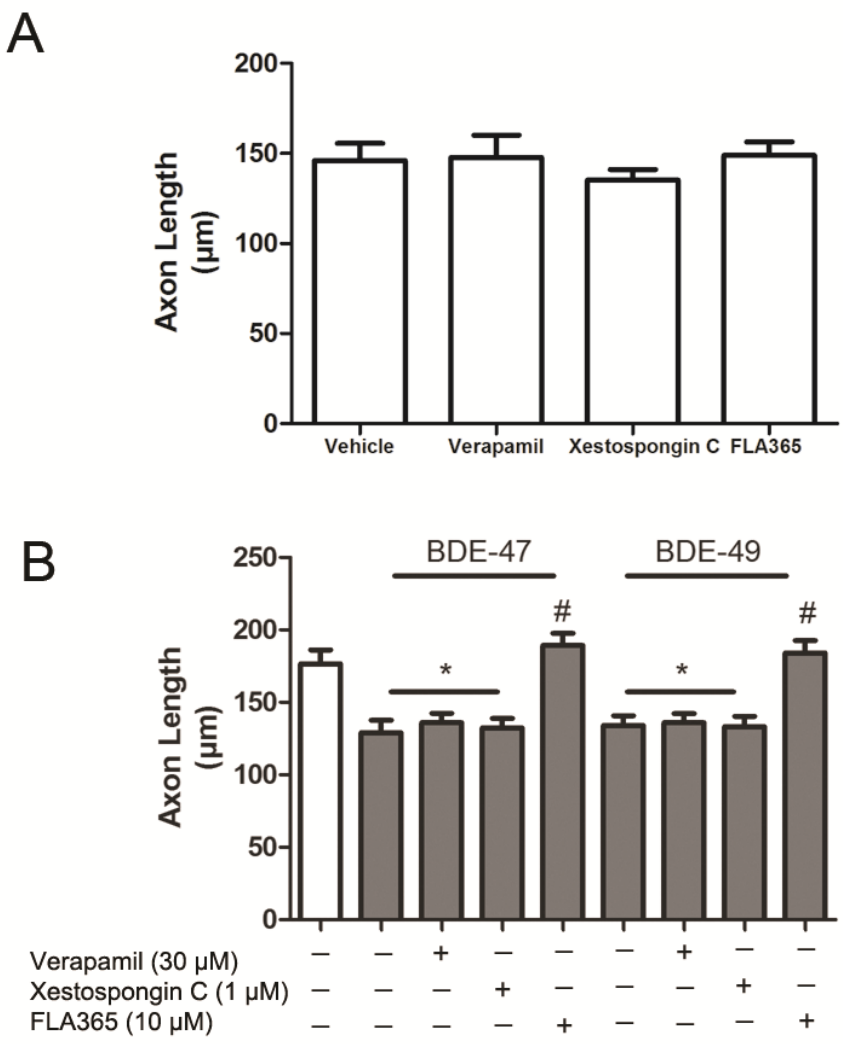

818

819 **Figure 7.**

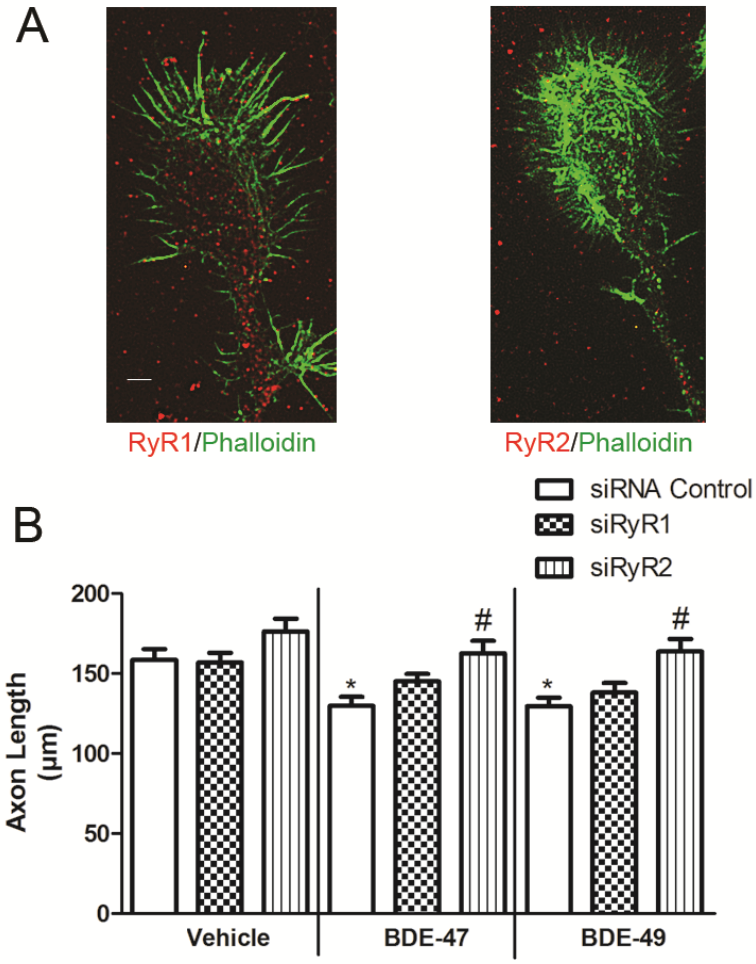

820

821 **Figure 8.**